International Journal of
Molecular Sciences

MDPI

Article

Beta-Adrenergic Activation of the Inward Rectifier K^+ Current Is Mediated by the CaMKII Pathway in Canine Ventricular Cardiomyocytes

Zsigmond Máté Kovács [1,†], Balázs Horváth [1,*,†], Csaba Dienes [1], József Óvári [1], Dénes Kiss [1], Tamás Hézső [1], Norbert Szentandrássy [1,2], János Magyar [1,3], Tamás Bányász [1,‡] and Péter Pál Nánási [1,4,‡]

[1] Department of Physiology, Faculty of Medicine, University of Debrecen, 4032 Debrecen, Hungary; kovacs.zsigmond@med.unideb.hu (Z.M.K.); dienes.csaba@med.unideb.hu (C.D.); ovari.jozsef@med.unideb.hu (J.Ó.); kiss.denes@med.unideb.hu (D.K.); hezso.tamas@med.unideb.hu (T.H.); szentandrassy.norbert@med.unideb.hu (N.S.); magyar.janos@med.unideb.hu (J.M.); banyasz.tamas@med.unideb.hu (T.B.); nanasi.peter@med.unideb.hu (P.P.N.)
[2] Department of Basic Medical Sciences, Faculty of Dentistry, University of Debrecen, 4032 Debrecen, Hungary
[3] Division of Sport Physiology, Department of Physiology, Faculty of Medicine, University of Debrecen, 4032 Debrecen, Hungary
[4] Department of Dental Physiology and Pharmacology, Faculty of Dentistry, University of Debrecen, 4032 Debrecen, Hungary
* Correspondence: horvath.balazs@med.unideb.hu
† These authors contributed equally to this work.
‡ These authors contributed equally to this work.

Abstract: Several ion currents in the mammalian ventricular myocardium are substantially regulated by the sympathetic nervous system via β-adrenergic receptor activation, including the slow delayed rectifier K^+ current and the L-type calcium current. This study investigated the downstream mechanisms of β-adrenergic receptor stimulation by isoproterenol (ISO) on the inward rectifier (I_{K1}) and the rapid delayed rectifier (I_{Kr}) K^+ currents using action potential voltage clamp (APVC) and conventional voltage clamp techniques in isolated canine left ventricular cardiomyocytes. I_{K1} and I_{Kr} were dissected by 50 μM $BaCl_2$ and 1 μM E-4031, respectively. Acute application of 10 nM ISO significantly increased I_{K1} under the plateau phase of the action potential (0–+20 mV) using APVC, and similar results were obtained with conventional voltage clamp. However, β-adrenergic receptor stimulation did not affect the peak current density flowing during terminal repolarization or the overall I_{K1} integral. The ISO-induced enhancement of I_{K1} was blocked by the calcium/calmodulin kinase II (CaMKII) inhibitor KN-93 (1 μM) but not by the protein kinase A inhibitor H-89 (3 μM). Neither KN-93 nor H-89 affected the I_{K1} density under baseline conditions (in the absence of ISO). In contrast, parameters of the I_{Kr} current were not affected by β-adrenergic receptor stimulation with ISO. These findings suggest that sympathetic activation enhances I_{K1} in canine left ventricular cells through the CaMKII pathway, while I_{Kr} remains unaffected under the experimental conditions used.

Keywords: inward rectifier K^+ current; rapid delayed rectifier K^+ current; sympathetic activation; protein kinase A; calcium/calmodulin-dependent protein kinase II; action potential voltage clamp; canine cardiomyocytes

check for updates

Citation: Kovács, Z.M.; Horváth, B.; Dienes, C.; Óvári, J.; Kiss, D.; Hézső, T.; Szentandrássy, N.; Magyar, J.; Bányász, T.; Nánási, P.P. Beta-Adrenergic Activation of the Inward Rectifier K^+ Current Is Mediated by the CaMKII Pathway in Canine Ventricular Cardiomyocytes. *Int. J. Mol. Sci.* **2024**, *25*, 11609. https://doi.org/10.3390/ijms252111609

Academic Editors: Ademuyiwa S. Aromolaran and Brian P. Delisle

Received: 25 September 2024
Revised: 16 October 2024
Accepted: 18 October 2024
Published: 29 October 2024

Copyright: © 2024 by the authors. Licensee MDPI, Basel, Switzerland. This article is an open access article distributed under the terms and conditions of the Creative Commons Attribution (CC BY) license (https://creativecommons.org/licenses/by/4.0/).

1. Introduction

Sympathetic activation of cardiac tissues is the primary mechanism by which the heart adapts to "fight-or-flight" situations. This leads to characteristic changes in contractility, calcium handling, and the morphology of the action potential, the latter due to modifications in underlying ion currents. Many cardiac ion currents, particularly the L-type calcium current ($I_{Ca,L}$) and the slow delayed rectifier potassium current (I_{Ks}), are robustly enhanced

by sympathetic stimulation through ß-adrenergic receptors. However, the effects of sympathetic stimulation on the ion currents that are responsible for the terminal repolarization of the action potential, such as the inward rectifier K^+ current (I_{K1}) and the rapid delayed rectifier K^+ current (I_{Kr}), remain poorly understood.

Isoproterenol (ISO, 1 μM), the well-known ß-adrenergic receptor agonist, suppressed I_{K1} in guinea pig ventricular myocytes [1] and canine Purkinje cells [2], while 10 nM ISO augmented I_{K1} in murine myocytes [3]. Not only are the effects inconsistent, but the underlying mechanisms are also controversial. According to the classic theory, most cardiac effects of catecholamines are mediated via the $ß_1$ receptor—cAMP—protein kinase A (PKA) pathway. However, the effect of PKA on I_{K1} remains disputed, as studies have shown that I_{K1} and Kir2.1 (KCNJ2) currents can either increase [4,5] or decrease [6,7] following PKA activation. Additionally, protein kinase C (PKC) activation generally appears to suppress I_{K1} [4,8] and its inhibition results in increased I_{K1} [9]. However, a different study reported that PKC activation increased I_{K1} [10].

I_{Kr} was increased in canine myocytes by ISO and PKA activators, an effect which was abolished in the presence of PKA inhibitors [11]. Similarly, ISO and the direct adenylyl cyclase activator forskolin increased I_{Kr} in guinea pig myocytes, effects which were sensitive to both PKA and PKC inhibition, as well as to a reduction in the intracellular calcium concentration ($[Ca^{2+}]_i$) caused by BAPTA-AM or nifedipine [12]. In contrast, both $ß_1$ receptor activation [13] and phosphodiesterase inhibition [14] decreased I_{Kr} and $K_v11.1$ (KCNH2; hERG) currents in a PKA-dependent mechanism in guinea pig myocytes.

Sympathetic activation raises $[Ca^{2+}]_i$, and Ca^{2+} ions may mediate certain effects of sympathetic activation in cardiac tissues through several mechanisms: (1) directly by themselves, (2) by forming complexes with Ca^{2+} binding proteins like calmodulin, and/or (3) via other Ca^{2+}-sensitive regulatory pathways, most notably the calcium/calmodulin-dependent protein kinase II (CaMKII). Previous studies have demonstrated that intracellular Ca^{2+} exerts a dynamic inhibitory effect on I_{K1} at positive voltages [15,16]. Therefore, an increase in $[Ca^{2+}]_i$ during sympathetic activation is expected to enhance the rectification of I_{K1}. Additionally, PKC might mediate indirect Ca^{2+}-dependent reduction of I_{K1}, because the activation of "conventional" Ca^{2+}-dependent PKC isoforms (e.g., PKCβ) has been reported to decrease the inward component of I_{K1} in Xenopus oocytes, in rat and mouse models [8,17], and in human atrial cells [8]. However, it remains unclear whether PKC affects the physiologically important outward component of the I_{K1} current.

Another indirect Ca^{2+}-dependent pathway, CaMKII, also influences I_{K1}. In murine myocytes, I_{K1} was reduced after CaMKII overexpression and increased following chronic CaMKII inhibition [18,19]. In rabbits, however, the overexpression of CaMKII led to an increase in I_{K1} [19]. The same study also found that acute activation of CaMKII increased the I_{K1} density in both rabbits and rats [19]. Similarly, in canine ventricular cells, I_{K1} was elevated following a rise in $[Ca^{2+}]_i$, but this effect was blocked by KN-93, a CaMKII inhibitor [20].

These findings suggest that the mechanisms by which sympathetic activation modulates I_{K1} and I_{Kr} in cardiac cells are still debated and appear to strongly depend on the specific experimental conditions and species studied. This complexity is further compounded by the known interaction between the PKA and CaMKII pathways [21]. Therefore, this study aims to disentangle the contributions of the PKA- and CaMKII-mediated mechanisms in the β-adrenergic regulation of I_{K1} and I_{Kr} in canine ventricular myocytes, with an experimental setting that closely mimics physiological conditions. This was achieved using the action potential voltage clamp (APVC) technique, keeping the intracellular Ca^{2+} homeostasis intact (without buffering $[Ca^{2+}]_i$) and applying a non-saturating concentration of the β-adrenergic agonist (10 nM ISO). Canine myocytes were selected for this study, because their electrophysiological properties closely resemble those of human ventricular cells [22–25].

2. Results

2.1. The Effect of β-Adrenergic Receptor Activation on I_{K1}

Parameters of I_{K1} were compared in five separate groups of myocytes under APVC conditions: (1) control (no treatment), (2) acute effect of 10 nM ISO, (3) acute effect of ISO in the presence of KN-93, (4) acute effect of ISO in the presence of H-89, and (5) acute effect of ISO in the presence of KN-93 + H-89. Figure 1 shows representative I_{K1} current traces obtained under these conditions. 10 nM ISO was used to achieve a biologically relevant moderate β-receptor activation, without receptor saturation.

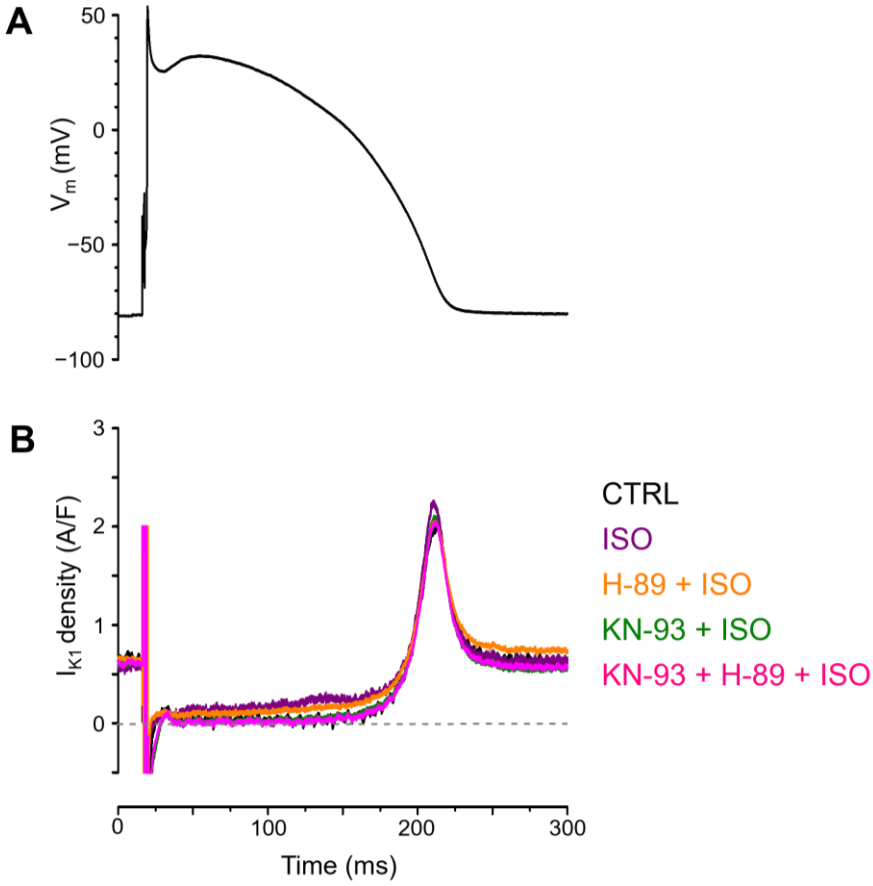

Figure 1. (**A**) Command action potential and (**B**) representative I_{K1} current traces obtained under APVC conditions in untreated control cells (CTRL), with ß-adrenergic stimulation in the presence of 10 nM ISO (ISO), ß-adrenergic stimulation following CaMKII inhibition with 1 μM KN-93 (KN-93 + ISO), ß-adrenergic stimulation following PKA inhibition with 3 μM H-89 (H-89 + ISO), and ß-adrenergic stimulation with the inhibition of both kinases (KN-93 + H-89 + ISO).

β-adrenergic receptor stimulation with ISO increased the mid-plateau density (current density measured at 50% of APD_{90}) of I_{K1} significantly (0.067 ± 0.019 A/F in control vs. 0.159 ± 0.029 A/F in ISO, n = 7 in both groups; Figure 2A). This effect of ISO was prevented by pretreatment with 1 μM KN-93 (CaMKII inhibitor; 0.073 ± 0.014 A/F, n = 7) but not by 3 μM H-89 (PKA inhibitor; 0.136 ± 0.024 A/F, n = 10), as also shown in Figure 2A. When the cells were pretreated with the combination of KN-93 and H-89, the mid-plateau density of I_{K1} (0.065 ± 0.013 A/F, n = 9) was similar to the value obtained either under control conditions or after KN-93 pretreatment alone. Interestingly, no significant effect of ISO was detected when either the peak value of I_{K1} (1.849 ± 0.120 A/F in control vs. 1.967 ± 0.159 A/F in ISO), measured during terminal repolarization, or the total current integral of I_{K1} (66.7 ± 4.4 mC/F in control vs. 77.7 ± 8.1 mC/F in ISO) was analyzed (Figures 1 and 2A–C).

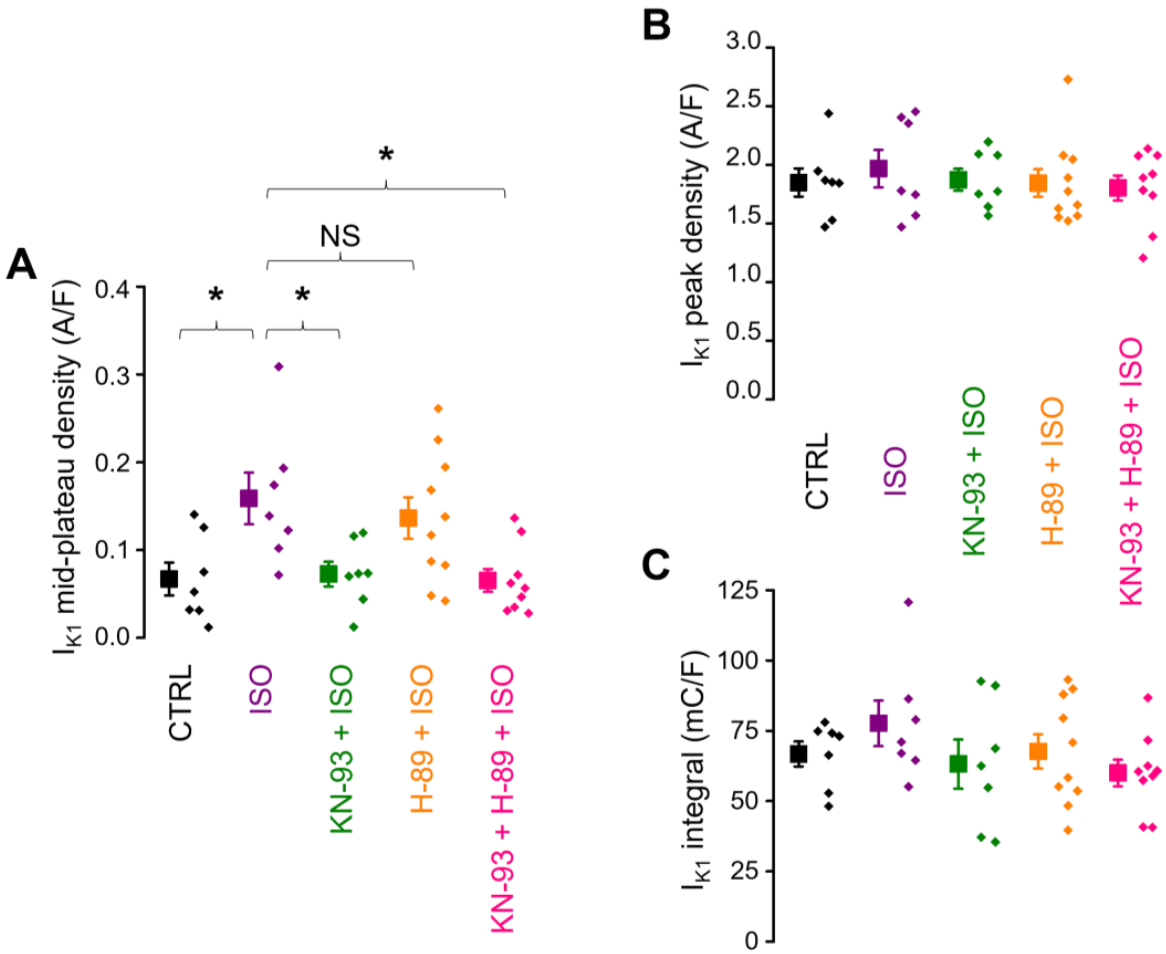

Figure 2. The effect of ß-adrenergic stimulation on I_{K1} and the suppressibility of this effect by CaMKII inhibition (KN-93) and PKA inhibition (H-89). Data obtained in 5 groups of myocytes are compared: untreated control (CTRL; n = 7/5), ß-adrenergic stimulation alone (ISO; n = 7/6), ß-adrenergic stimulation following CaMKII inhibition (KN-93 + ISO; n = 7/6), ß-adrenergic stimulation following PKA inhibition (H-89 + ISO; n = 10/7), and ß-adrenergic stimulation with the inhibition of both kinases (KN-93 + H-89 + ISO; n = 9/7). The "n" numbers in parentheses indicate the number of cells over the number of animals used in that experimental group. (**A**) Mid-plateau current densities, (**B**) peak current densities, (**C**) current integrals. Symbols and bars are mean ± SEM, and small dots represent individual data. Asterisks (*) indicate significant differences ($p < 0.05$) between groups. NS: not significant.

These results indicate that the β-adrenergic-pathway-mediated augmentation of I_{K1} appears during the plateau of the AP; therefore, the density of I_{K1} was analyzed at two fixed membrane potential levels of +20 mV and 0 mV. The former is close to the mid-plateau potential, while the latter overlaps with a more accelerated level of repolarization (Figure 3A). As shown in the panels in Figure 3B,C, the pattern is identical to the one seen in Figure 2, i.e., the I_{K1} density was significantly larger in ISO (0.148 ± 0.034 A/F at +20 mV, 0.202 ± 0.041 A/F at 0 mV) compared to control conditions (0.042 ± 0.011 A/F and 0.090 ± 0.018 A/F, respectively), while this effect of ISO was prevented by KN-93 (0.052 ± 0.012 A/F and 0.095 ± 0.028 A/F, respectively) but not by H-89 (0.127 ± 0.025 A/F and 0.159 ± 0.022 A/F, respectively).

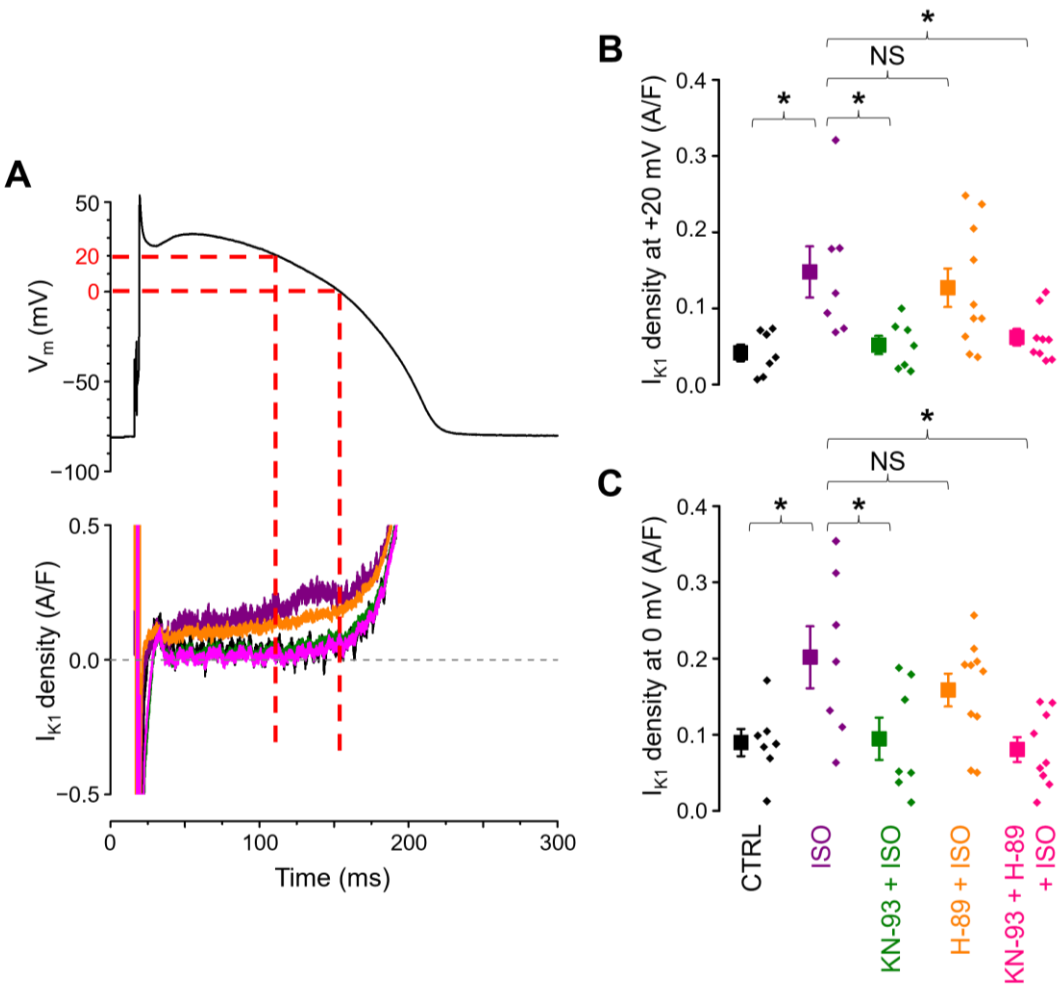

Figure 3. (**A**) Command action potential (above) and representative enlarged I_{K1} current traces flowing during the action potential plateau (below). Dashed lines indicate the corresponding voltage and current values at 0 mV and at +20 mV. (**B**,**C**) I_{K1} densities measured at +20 mV and at 0 mV, respectively, in the 5 cell groups of control (CTRL; n = 7/5), ß-adrenergic stimulation alone (ISO; n = 7/6), ß-adrenergic stimulation following CaMKII inhibition (KN-93 + ISO; n = 7/6), ß-adrenergic stimulation following PKA inhibition (H-89 + ISO; n = 10/7), and ß-adrenergic stimulation with the inhibition of both kinases (KN-93 + H-89 + ISO; n = 9/7). The "n" numbers in parentheses indicate the number of cells over the number of animals used in that experimental group. Symbols and bars are mean ± SEM, and small dots represent individual data. Asterisks (*) indicate significant differences ($p < 0.05$) between groups. NS: not significant.

Similar results were obtained when the effects of ISO alone and in the presence of KN-93 or H-89 on I_{K1} density were studied under conventional voltage clamp conditions at test potentials ranging from −80 mV to +20 mV. Compared to the control cells, the I_{K1} density was significantly larger in ISO in the range of −30 mV to +20 mV, an effect which was abolished by CaMKII blockade with KN-93 but not by PKA inhibition with H-89 (Figure 4A–C). At 0 mV, the I_{K1} current densities were 0.266 ± 0.042 A/F in control conditions (n = 11), 0.525 ± 0.073 A/F in ISO-pretreated cells (n = 9), 0.211 ± 0.067 A/F in KN-93 + ISO (n = 10), and 0.431 ± 0.103 A/F in H-89 + ISO (n = 9), as illustrated in Figure 4C. No significant differences between the cell groups were observed at membrane potentials below −30 mV.

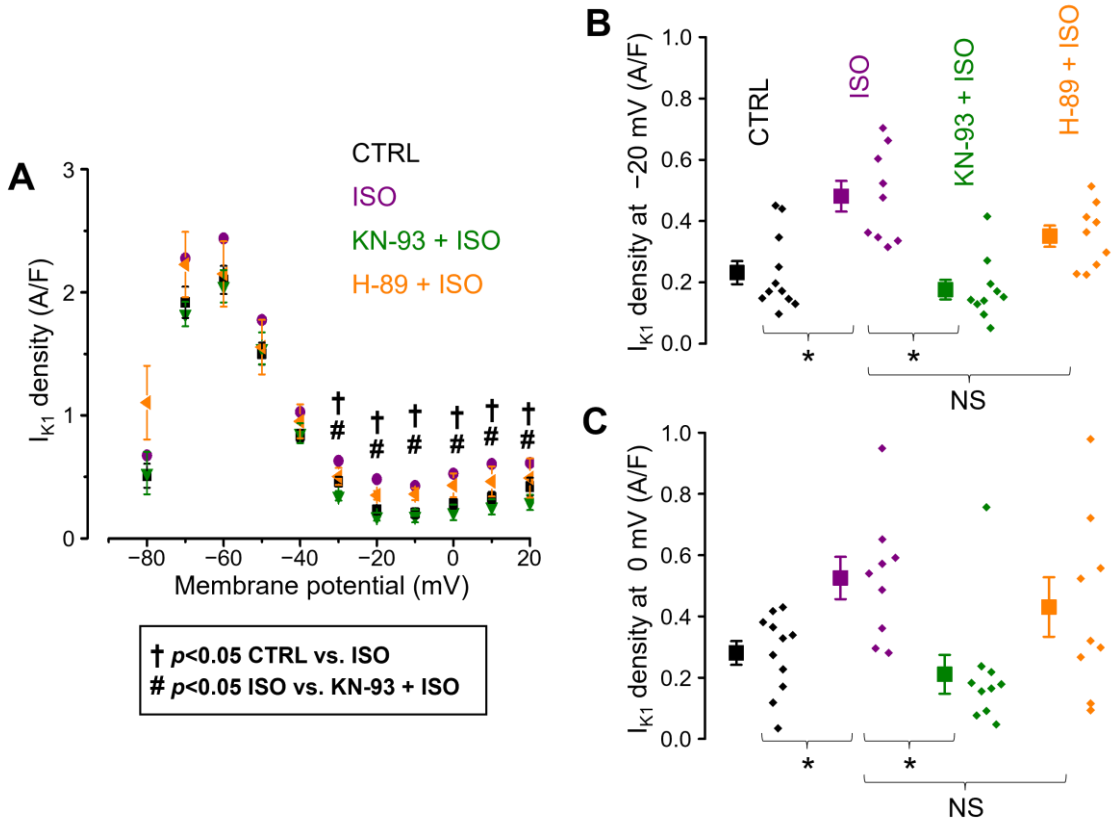

Figure 4. The effects of ISO alone and in the presence of KN-93 and H-89 on the I_{K1} density under conventional voltage clamp conditions. (**A**) I_{K1} densities measured at the end of various test potentials (shown on the abscissa) lasting for 250 ms and rising from the holding potential of −80 mV in the 4 cell groups of control (CTRL; n = 11/3), ß-adrenergic stimulation alone (ISO; n = 9/5), ß-adrenergic stimulation following CaMKII inhibition (KN-93 + ISO; n = 10/3), and ß-adrenergic stimulation following PKA inhibition (H-89 + ISO; n = 9/5). The "n" numbers in parentheses indicate the number of cells over the number of animals used in that experimental group. Detailed statistical analyses of the I_{K1} densities measured at −20 mV and 0 mV are depicted in panels (**B**) and (**C**), respectively. Symbols and bars are mean ± SEM, and small dots represent individual data. On panel (**A**), daggers (†) and hash signs (#) indicate significant differences ($p < 0.05$) between the control and ISO groups and between the ISO and KN-93 + ISO groups, respectively. On panels (**B**,**C**), asterisks (*) indicate significant differences ($p < 0.05$) between groups. NS: not significant.

2.2. Effects of PKA and CaMKII Inhibition on I_{K1} Without β-Adrenergic Receptor Stimulation

The effects of KN-93 and H-89 on I_{K1} were also studied under baseline conditions, without β-adrenergic receptor activation. No differences were observed in the mid-plateau density, peak current density, or current integral between the untreated group and those exposed to KN-93 or H-89 (Figure 5A–D).

2.3. I_{Kr} Is Not Affected by β-Adrenergic Receptor Stimulation, PKA Inhibition, or CaMKII Inhibition

The consequences of KN-93 and H-89 treatment, as well as the effects of ISO in the absence and presence of these inhibitors, were studied on I_{Kr} under similar experimental conditions. Neither ISO, nor the inhibitors applied alone or in combination with ISO, modified the profile (Figure 6A), the mid-plateau density (Figure 6B), the peak density (Figure 6C), and the integral (Figure 6D) of I_{Kr}.

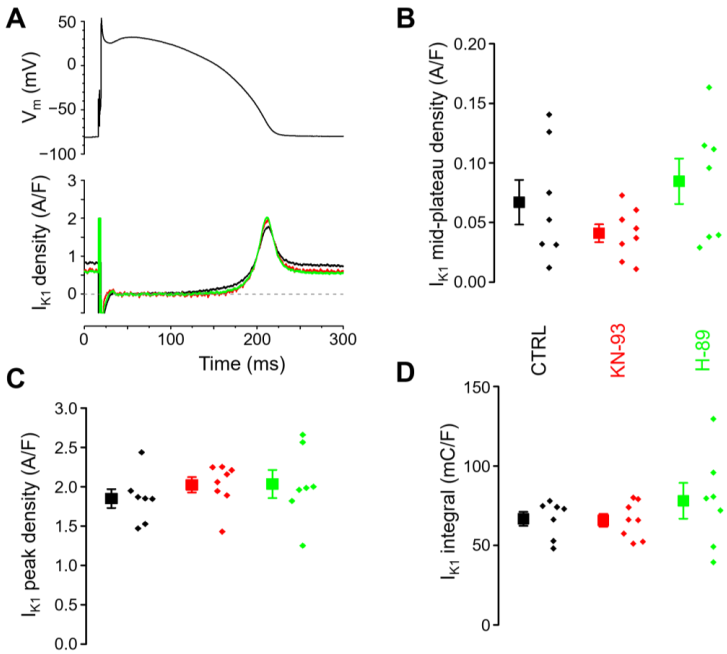

Figure 5. CaMKII inhibition with KN-93 or PKA inhibition with H-89 has no effect on I_{K1} under baseline conditions. The cell groups of control (CTRL; n = 7/5), CaMKII inhibition (KN-93; n = 8/5), and PKA inhibition (H-89; n = 7/4) were compared. The "n" numbers in parentheses indicate the number of cells over the number of animals used in that experimental group. (**A**) Command action potential (above) and the corresponding representative I_{K1} current traces flowing during the action potential (below). (**B**) Mid-plateau current densities, (**C**) peak current densities, and (**D**) current integrals. Symbols and bars are mean ± SEM, and small dots represent individual data. The arithmetic means of the groups were not significantly different in any parameters with one-way ANOVA.

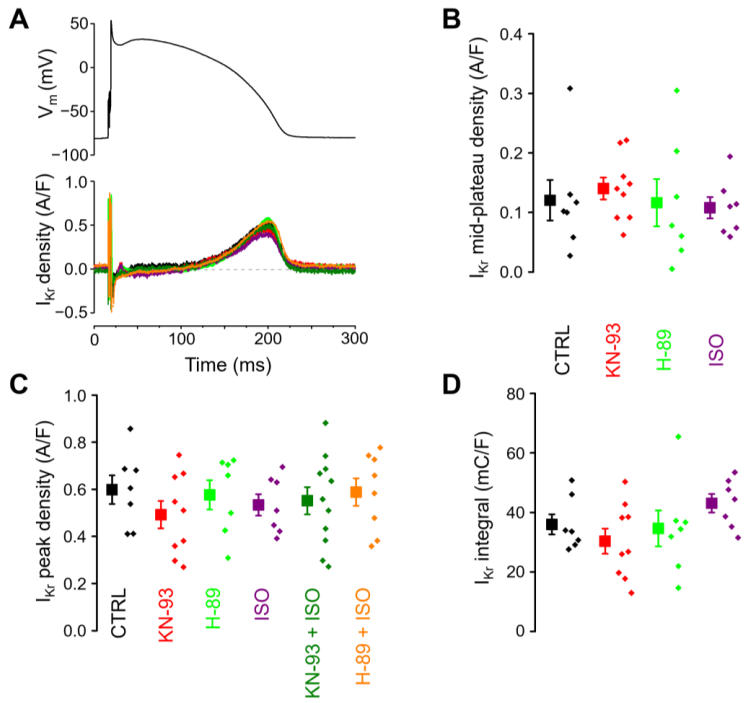

Figure 6. The effects of PKA and CaMKII inhibition with or without ß -adrenergic receptor activation on I_{Kr}. The cell groups of control (CTRL; n = 7/5), CaMKII inhibition under baseline conditions (KN-93; n = 9/5), PKA inhibition under baseline conditions (H-89; n = 7/4), ß-adrenergic stimulation alone (ISO; n = 7/6), ß-adrenergic stimulation following CaMKII inhibition (KN-93 + ISO; n = 11/6),

and ß-adrenergic stimulation following PKA inhibition (H-89 + ISO; n = 8/6). The "n" numbers in parentheses indicate the number of cells over the number of animals used in that experimental group. (**A**) Command action potential (above) and the corresponding representative I_{Kr} current profiles flowing during the action potential (below). (**B**) Mid-plateau current densities, (**C**) peak current densities, and (**D**) current integrals. Symbols and bars are mean ± SEM, and small dots represent individual data. The arithmetic means of the groups were not significantly different in any parameters with one-way ANOVA.

3. Discussion

In the present study, the effect of 10 nM ISO, corresponding to a moderate sympathetic activation of the heart, was studied on two K^+ currents governing terminal repolarization: I_{K1} and I_{Kr}. I_{K1} was increased by ISO in the plateau phase of the canine ventricular AP, while I_{Kr} was not influenced by ISO. This is the first study to demonstrate that the β-adrenergic-pathway-dependent augmentation of the canine I_{K1} is not mediated by the PKA pathway, since the ISO effect was not prevented by pretreatment with the PKA inhibitor H-89. In contrast, the CaMKII inhibitor KN-93 abolished the effect of ISO on I_{K1}, indicating that CaMKII is responsible for the effect. No synergy was observed in the contribution of CaMKII and PKA, since the I_{K1} densities measured in the presence of ISO + KN-93 and ISO + KN-93 + H-89 were not different. Also, the baseline activity of CaMKII or PKA is not involved in the regulation of I_{K1}, since neither KN-93 alone nor H-89 alone modulated the density of I_{K1} under baseline conditions.

To explain our findings, there are two plausible possibilities based on experimental data in the literature. ß-adrenergic activation increases CaMKII activity in guinea pig cardiomyocytes through a nitric oxide (NO)-dependent, but cAMP-independent, pathway [26]. Based on this, the authors concluded that the ß-adrenergic receptor stimulation may activate CaMKII by a novel direct pathway involving nitrogen oxide synthase. Indeed, NO increased CaMKII activity in human atrial myocytes and $K_{ir}2.1$ currents [27], and nitrosylation of CaMKII-delta has been shown to mediate the effect of 100 nM ISO in murine cardiac cells [28]. The involvement of the guanine nucleotide exchange protein activated by cAMP (EPAC) in the stimulation of CaMKII has also been reported [29–31]. It has been suggested that the NO-dependent activation of CaMKII is mediated by an EPAC-related pathway in murine and rabbit myocytes via a cAMP → EPAC → NO → CaMKII sequence [32]. Alternatively, the activation of CaMKII may be mediated by a cAMP→ EPAC → Rap → PLC-epsilon sequence [30]. Furthermore, the contribution of ß-arrestins and related signalosomes cannot be excluded either [33]. Further studies are required to identify the exact signal transduction mechanism(s) in canine ventricular cells mediating ß-adrenergic regulation of I_{K1}.

It was unexpected to find that ISO only increased I_{K1} in the plateau voltage range of the AP but not at more negative voltages, such as during the terminal repolarization, when the current density is maximal. This suggests that the maximal overall K^+ conductance was unaffected by ß-adrenergic activation. It is likely that the number of active Kir2.1 channels and their maximal conductance remained unchanged, although two opposing effects — such as an increased conductance but decreased Kir2.x channel expression — could also explain this observation. Our results suggest that CaMKII-induced phosphorylation may reduce the inward-going rectification of I_{K1}, resulting in a larger outward I_{K1} current at positive membrane potentials, as seen in our experiments. A similar phosphorylation-dependent alteration in the rectification of Kir2.1/KCNJ2 channels has been reported by Kalscheur et al. in an R67Q mutant channel [5]. In wild-type Kir2.1 channels, the phosphorylation of the channel on Ser425 increases I_{K1}, an effect which is lost in the R67Q mutants. The authors attributed this to an increased I_{K1} "rectification index" [5]. As the AP duration is most sensitive to changes in the net membrane current when the repolarization is slow [34], such as during the AP plateau phase, even a small increase in I_{K1} under the AP plateau can significantly shorten the AP.

In agreement with our results, Nagy et al. [20] also reported a CaMKII-mediated $[Ca^{2+}]_i$-dependent I_{K1} augmentation in a wide range of membrane voltages in canine ventricular cells. However, there is an apparent contradiction between the results of the two studies regarding the peak I_{K1} density. Nagy et al. reported a significantly larger peak I_{K1} density under APVC conditions in case of larger $[Ca^{2+}]_i$ (attributed to CaMKII activation), whereas we found no significant effect of ISO on the peak I_{K1} density. These contradictory results may originate from the slightly different experimental conditions. In their canine APVC studies, Nagy et al. set the $[Ca^{2+}]$ of the pipette solutions with BAPTA and $CaCl_2$ to low (~160 nM) and high (~900 nM) levels to elucidate the $[Ca^{2+}]_i$ dependency of I_{K1}, whereas we used adrenergic stimulation to achieve CaMKII activation, with no Ca^{2+} buffers applied.

In rabbit ventricular cells, under experimental conditions quite similar to ours, Hegyi et al. [35] found that the inhibition of CaMKII did not alter I_{K1} parameters, and the application of 10 nM ISO did not affect the peak I_{K1} density when intracellular calcium homeostasis was preserved, results which are in good agreement with our data (Figures 2B and 5). In the study by Hegyi et al., however, 10 nM ISO increased the I_{K1} net charge significantly (by 23%) compared to control conditions. The same comparison did not reach statistical significance in our dataset, although 10 nM ISO-treated cells had an approximately 16% (11 mC/F) larger I_{K1} integral compared to the control cells (Figure 2C). The authors [35] did not specifically comment on which part of the I_{K1} current trace became larger to cause the significant increase in the I_{K1} integral. Since the peak I_{K1} did not change, the most plausible explanation is a significant increase in I_{K1} under the plateau phase, just like what we found in the present study. When $Ca^{2+}{}_i$ was buffered with BAPTA, the authors found no significant differences in either the I_{K1} peak or I_{K1} net charge between basal conditions and ß-adrenergic stimulation with 10 nM ISO. In our study, KN-93 had a similar effect, preventing the ISO-induced increase in I_{K1} under the AP plateau (Figures 3B,C and 4B,C). Furthermore, cells in the control and KN-93 + ISO groups had similar I_{K1} integrals (66.7 ± 4.4 mC/F and 63.2 ± 8.7 mC/F, respectively) that were considerably (respectively, around 16% and 23%) smaller than in the ISO-treated cells (77.7 ± 8.1 mC/F), but these differences in the net charge carried by I_{K1} did not reach statistical significance. The observations of both studies can be explained if we accept that ß-adrenergic receptor activation increases CaMKII activity, and in turn, CaMKII upregulates the I_{K1} current. Therefore, if CaMKII activation is prevented either by $Ca^{2+}{}_i$ buffering, or by direct CaMKII inhibition, I_{K1} upregulation is abolished.

It is well established that I_{K1} is substantially activated by phosphatidylinositol 4,5-bisphosphate (PIP_2) [36,37], and that β-adrenergic receptor activation leads to increased PIP_2 levels [38]. In the latter article by Xu et al., the authors suggest that the β-adrenergic receptor activation raises the PIP_2 levels because of the PKA-dependent phosphorylation and subsequent activation of phosphatidylinositol-4-phosphate 5-kinase gamma (PIP5Kγ). However, Xu et al. applied *30 μM H-89 extracellularly* to inhibit PKA. Notably, H-89 is a potent and selective inhibitor of β_1 (and β_2) adrenergic receptor ligand binding with an approximate K_i of 350 nM (and 180 nM) on human airway smooth muscle cells [39]. This β-receptor inhibitor property must be considered when applying H-89 extracellularly. Therefore, the results that Xu et al. show in Figure 4B [38] can be attributed to *β-adrenergic receptor inhibition by H-89*. This was also the reason why we used a lower concentration of H-89 (3 μM) *in the pipette solution*. Considering all of these, an alternative explanation for our findings is possible, besides the suggested CaMKII-dependent phosphorylation of Kir channels. As β-adrenergic receptor activation increases PIP_2 levels [38], it could also enhance I_{K1} through this mechanism. Since in our experiments, intracellularly applied KN-93 prevented the augmentation of I_{K1}, but H-89 did not have such an effect, this putative mechanism is clearly not mediated by PKA, and CaMKII might play a role in it.

In contrast to our findings on I_{K1}, and previous studies on both I_{Ks} [40,41] and I_{K1} [1–3], the I_{Kr} density was not altered by ß-adrenergic activation in our study, nor was it sensitive to the inhibition of either CaMKII or PKA under our experimental conditions. In rabbit

ventricular cells under APVC conditions and in normal intracellular calcium homeostasis, similar to our experimental settings, CaMKII inhibition did not alter I_{Kr} parameters either, whereas ß-adrenergic stimulation with 10 nM ISO caused an 8.1% increase in the peak I_{Kr} density and a 23.1% increase in the current integral [35]. In guinea pig myocytes, I_{Kr} was increased by PKC activation [12] but suppressed by PKA activation [13]. In contrast, PKA activation increased the I_{Kr} amplitude in canine myocytes [11], while it decreased it in human and rat myocytes [8,9]. Since both the PKA- and PKC-related pathways are $[Ca^{2+}]_i$-dependent, it is not surprising that these effects were strongly influenced by the $[Ca^{2+}]_i$ levels [12]. Similarly, ISO increased the I_{Kr} density when $[Ca^{2+}]_i$ was kept low ($[Ca^{2+}]_i$ was buffered by EGTA, and Ca^{2+} entry was blocked by nifedipine) in conventional voltage clamp experiments [11] but was not altered in the present study when the Ca^{2+} homeostasis was intact and experiments were carried out in APVC conditions. These findings together suggest that ß-adrenergic stimulation might modify I_{Kr} in the canine heart, but likely through two opposing pathways, which may cancel each other out under intact intracellular Ca^{2+} homeostasis. Further investigations are necessary to clarify the exact role of these mechanisms.

4. Materials and Methods

4.1. Animals

Adult mongrel dogs of both sexes were anesthetized using intramuscular injections of 10 mg/kg ketamine hydrochloride (Calypsol, Richter Gedeon, Budapest, Hungary) +1 mg/kg xylazine hydrochloride (Sedaxylan, Eurovet Animal Health BV, Bladel, The Netherlands) according to the protocol approved by the local Animal Care Committee of the University of Debrecen (license N°: 9/2015/DEMÁB). All animal procedures conform to the guidelines laid down in the Declaration of Helsinki in 1964 and its later amendments, and to the Guide to the Care and Use of Experimental Animals (Vol. 1, 2nd ed., 1993, and Vol. 2, 1984, Canadian Council on Animal Care).

4.2. Isolation of Cardiomyocytes

Single canine myocytes were obtained by enzymatic dispersion using the segment perfusion technique, as previously described [34,42]. A wedge-shaped section of the ventricular wall, supplied by the left anterior descending coronary artery, was cannulated and perfused with a nominally Ca^{2+}-free Joklik solution (Minimum Essential Medium Eagle, Joklik Modification). After washing out the blood (5 min) using this solution, it was supplemented with 1 mg/mL collagenase (Type II, Worthington Biochemical Co., Lakewood, NJ, USA; representing final activity of 224 U/mL) and 0.2% bovine serum albumin (Fraction V.) containing 50 μM Ca^{2+}. This perfusion typically lasted for 30 min. Following this period, the tissue was minced, and the cells were released by gentle agitation. Finally, the normal external Ca^{2+} concentration was gradually restored. The cells were stored in Minimum Essential Medium Eagle at 15 °C before use. This protocol yielded myocytes showing clear cross-striations, dominantly of a midmyocardial origin.

4.3. Electrophysiology

Cells were superfused in a plexiglass chamber under an inverted microscope with a modified Tyrode solution by gravity flow at a rate of 1–2 mL/min. This superfusate contained NaCl, 121; KCl, 4; $CaCl_2$, 1.3; $MgCl_2$, 1; HEPES, 10; $NaHCO_3$, 25; and glucose, 10 (mM) at pH = 7.35 with an osmolarity of 300 mOsm. The bath temperature was set to 37 °C using a temperature controller (Cell MicroControls, Norfolk, VA, USA). Electrical signals were amplified and recorded (MultiClamp 700A or 700B, Molecular Devices, Sunnyvale, CA, USA) under the control of a pClamp software (version 10.6, Molecular Devices) following analog–digital conversion (Digidata 1440A or 1332, Molecular Devices). Electrodes with tip resistances of 2–3 MΩ when filled with pipette solution were made from borosilicate glass. The pipette solution contained K-aspartate, 120; KCl, 30; KOH, 10; MgATP, 3; HEPES, 10; Na_2-phosphocreatine, 3; EGTA, 0.01; and cAMP, 0.002 at

pH = 7.3 and osmolality of 285 mOsm. The series resistance was kept between 4 and 8 MΩ. The experiment was discarded when the series resistance changed substantially during the measurement. After establishing the whole-cell configuration, cells were continuously paced in current-clamp mode for at least 10 min at a cycle length of 0.7 s, corresponding to the normal heart rate of dogs. See further details in [25,43].

The experiments were performed using the APVC technique according to the method previously described [24,44,45]. To avoid the consequences of cell-to-cell variations in AP configurations, measurements were performed using a "canonic" AP as a command signal instead of the own AP of the cell. This canonic AP was a representative midmyocardial canine AP with average parameters. Cells were paced with the "canonic" AP at a cycle length of 0.7 s. The application of uniform command APs allowed for the comparison of the individual current traces. I_{K1} was dissected by 50 μM $BaCl_2$, applied after pretreatment with 1 μM E-4031 plus 0.5 μM HMR-1556 to block I_{Kr} and I_{Ks}, respectively. When measuring I_{Kr} as a 1 μM E-4031 sensitive current, the cells were pretreated with 0.5 μM HMR-1556 to block I_{Ks}. Before and after 5 min of superfusion with the inhibitor ($BaCl_2$ for I_{K1} or E-4031 for I_{Kr}), 20 consecutive current traces were recorded and averaged in order to reduce noise and trace-to-trace fluctuations. The drug-sensitive current was obtained by subtracting the averaged post-drug current trace from the averaged pre-drug one. These dissected currents were evaluated by determining their maximal amplitudes (peak currents), their amplitudes measured at the half-duration of the command AP (mid-plateau current amplitudes), and the total charge carried by the current (current integrals). All these parameters were normalized to cell capacitance, which was calculated based on hyperpolarizing the cells from +10 mV to −10 mV for 15 ms.

Conventional voltage clamp experiments of I_{K1} (shown in Figure 4) were performed with the same pipette solution as the APVC measurements. For these experiments, the bath solution was supplemented with 1 μM E-4031 and 0.5 μM HMR-1556 for I_{Kr} and I_{Ks} blockade, respectively. The steady-state I_{K1} was defined as the $BaCl_2$-sensitive current. To obtain current traces, 250 ms long voltage test pulses were delivered in 10 mV increments from the holding potential of −80 mV at a rate of 1 Hz. After applying 50 μM $BaCl_2$ for 5 min, the recording was repeated, and these current traces were subtracted from their respective pre-$BaCl_2$ ones. $BaCl_2$-sensitive current readings from the last 5 ms of the test pulses were averaged, normalized to the cell capacitance, plotted against their respective test potentials, and regarded as the I_{K1} current densities.

4.4. Chemicals

Chemicals were purchased from Sigma-Aldrich (St. Louis, MO, USA), except for HMR-1556, KN-93, and H-89, which were purchased from Tocris Bioscience (Bristol, UK). An ISO stock solution of 10 μM was freshly created right before each experiment, and this was diluted to a 10 nM final concentration in the bath solution. ISO application started 5 min before the start of APVC experiments, and from that time point, it was continuously perfused in the bath. Besides ISO, the potassium channel inhibitors HMR-1556, E-4031, and $BaCl_2$ were also used in the bath solution.

When applied extracellularly, 1 μM KN-93 has been shown to abolish I_{Kr} in rabbit and guinea pig ventricular myocytes [46], whereas H-89 is shown to be a potent and selective inhibitor of β_1 and β_2 adrenergic receptor ligand binding with respective K_i values of around 350 nM and 180 nM on human airway smooth muscle cells [39]. Therefore, both kinase inhibitors (1 μM KN-93 and 3 μM H-89) were applied in the pipette solution.

4.5. Statistics

Results are expressed as mean ± SEM values, and "*n*" denotes the number of myocytes studied. The experimental groups were statistically compared with one-way ANOVA, followed by Dunnett's post hoc test if the ANOVA yielded significant results. In the results presented in Figures 2–4, the 10 nM ISO-treated group served as the reference group, whereas in the comparisons shown in Figures 5 and 6, all other groups were compared

to the untreated "control" group in Dunnett's post hoc test. Differences were considered statistically significant when p was less than 0.05.

Author Contributions: Conceptualization: B.H., T.B., and P.P.N.; Cell isolation: Z.M.K., C.D., J.Ó., D.K., and T.H.; Action potential voltage clamp recordings: Z.M.K., B.H., C.D., J.Ó., D.K., T.H., and N.S.; Voltage clamp recordings: Z.M.K., B.H., C.D., J.Ó., and N.S.; Data analysis: Z.M.K., B.H., J.M., N.S., and T.B.; Writing—original draft preparation: P.P.N., B.H., and Z.K; Writing—review and editing: B.H., T.B., and P.P.N.; Visualization: Z.M.K., B.H., and J.M.; Funding acquisition: P.P.N., N.S., and T.B. All authors have read and agreed to the published version of the manuscript.

Funding: This work was funded by the National Research Development and Innovation Office (NKFIH-K138090 to PPN, NKFIH-K142764 to NS and NKFIH-K147301 to TB, EKÖP-24-4-I-DE-455 to ZK, EKÖP-24-3-II-DE-154 to JO). The work was supported by the University of Debrecen Program for Scientific Publication (NS, BH).

Institutional Review Board Statement: The study was conducted according to the guidelines of the Declaration of Helsinki and approved by the Institutional Review Board (or Ethics Committee) of University of Debrecen (license No: 9/2015/DEMÁB, date of approval: 22 December 2015).

Informed Consent Statement: Not applicable.

Data Availability Statement: Data are available upon reasonable request. Inquiries regarding research data should be directed to the corresponding author.

Acknowledgments: The authors thank Éva Sági for her excellent technical assistance.

Conflicts of Interest: The authors declare no conflicts of interest.

Abbreviations

AP	action potential
APVC	action potential voltage clamp
$[Ca^{2+}]_i$	intracellular Ca^{2+} concentration
CaMKII	calcium/calmodulin-dependent protein kinase II
EPAC	guanine nucleotide exchange protein activated by cAMP
hERG	voltage-gated potassium channel subfamily H member 2
$I_{Ca,L}$	L-type Ca^{2+} current
I_{K1}	inward rectifier K^+ current
I_{Kr}	rapid delayed rectifier K^+ current
I_{Ks}	slow delayed rectifier K^+ current
ISO	Isoproterenol
KCNH2	voltage-gated potassium channel subfamily H member 2
KCNJ2	inward rectifier potassium channel subfamily J member 2
Kir2.1	inward rectifier potassium channel subfamily J member 2
Kv11.1	voltage-gated potassium channel subfamily H member 2
NO	nitric oxide
PIP_2	phosphatidylinositol 4,5-bisphosphate
PKA	protein kinase A
PKC	protein kinase C

References

1. Koumi, S.; Wasserstrom, J.A.; Ten Eick, R.E. Beta-adrenergic and cholinergic modulation of inward rectifier K^+ channel function and phosphorylation in guinea-pig ventricle. *J. Physiol.* **1995**, *486 Pt 3*, 661–678. [CrossRef] [PubMed]
2. Tromba, C.; Cohen, I.S. A novel action of isoproterenol to inactivate a cardiac K^+ current is not blocked by beta and alpha adrenergic blockers. *Biophys. J.* **1990**, *58*, 791–795. [CrossRef] [PubMed]
3. Reilly, L.; Alvarado, F.J.; Lang, D.; Abozeid, S.; Van Ert, H.; Spellman, C.; Warden, J.; Makielski, J.C.; Glukhov, A.V.; Eckhardt, L.L. Genetic Loss of I(K1) Causes Adrenergic-Induced Phase 3 Early Afterdepolariz ations and Polymorphic and Bidirectional Ventricular Tachycardia. *Circ. Arrhythm. Electrophysiol.* **2020**, *13*, e008638. [CrossRef] [PubMed]
4. Fakler, B.; Brandle, U.; Glowatzki, E.; Zenner, H.P.; Ruppersberg, J.P. Kir2.1 inward rectifier K^+ channels are regulated independently by protein kinases and ATP hydrolysis. *Neuron* **1994**, *13*, 1413–1420. [CrossRef]

5. Kalscheur, M.M.; Vaidyanathan, R.; Orland, K.M.; Abozeid, S.; Fabry, N.; Maginot, K.R.; January, C.T.; Makielski, J.C.; Eckhardt, L.L. KCNJ2 mutation causes an adrenergic-dependent rectification abnormality with calcium sensitivity and ventricular arrhythmia. *Heart Rhythm* **2014**, *11*, 885–894. [CrossRef]
6. Vega, A.L.; Tester, D.J.; Ackerman, M.J.; Makielski, J.C. Protein kinase A-dependent biophysical phenotype for V227F-KCNJ2 mutation in catecholaminergic polymorphic ventricular tachycardia. *Circ. Arrhythm. Electrophysiol.* **2009**, *2*, 540–547. [CrossRef]
7. Wischmeyer, E.; Karschin, A. Receptor stimulation causes slow inhibition of IRK1 inwardly rectifying K^+ channels by direct protein kinase A-mediated phosphorylation. *Proc. Natl. Acad. Sci. USA* **1996**, *93*, 5819–5823. [CrossRef]
8. Karle, C.A.; Zitron, E.; Zhang, W.; Wendt-Nordahl, G.; Kathofer, S.; Thomas, D.; Gut, B.; Scholz, E.; Vahl, C.F.; Katus, H.A.; et al. Human cardiac inwardly-rectifying K^+ channel Kir(2.1b) is inhibited by direct protein kinase C-dependent regulation in human isolated cardiomyocytes and in an expression system. *Circulation* **2002**, *106*, 1493–1499. [CrossRef]
9. Fauconnier, J.; Lacampagne, A.; Rauzier, J.M.; Vassort, G.; Richard, S. Ca^{2+}-dependent reduction of IK1 in rat ventricular cells: A novel paradigm for arrhythmia in heart failure? *Cardiovasc. Res.* **2005**, *68*, 204–212. [CrossRef]
10. Scherer, D.; Kiesecker, C.; Kulzer, M.; Gunth, M.; Scholz, E.P.; Kathofer, S.; Thomas, D.; Maurer, M.; Kreuzer, J.; Bauer, A.; et al. Activation of inwardly rectifying Kir2.x potassium channels by beta 3-adrenoceptors is mediated via different signaling pathways with a predominant role of PKC for Kir2.1 and of PKA for Kir2.2. *Naunyn-Schmiedeberg's Arch. Pharmacol.* **2007**, *375*, 311–322. [CrossRef]
11. Harmati, G.; Banyasz, T.; Barandi, L.; Szentandrassy, N.; Horvath, B.; Szabo, G.; Szentmiklosi, J.A.; Szenasi, G.; Nanasi, P.P.; Magyar, J. Effects of beta-adrenoceptor stimulation on delayed rectifier K(+) currents in canine ventricular cardiomyocytes. *Br. J. Pharmacol.* **2011**, *162*, 890–896. [CrossRef] [PubMed]
12. Heath, B.M.; Terrar, D.A. Protein kinase C enhances the rapidly activating delayed rectifier potassium current, IKr, through a reduction in C-type inactivation in guinea-pig ventricular myocytes. *J. Physiol.* **2000**, *522 Pt 3*, 391–402. [CrossRef] [PubMed]
13. Karle, C.A.; Zitron, E.; Zhang, W.; Kathofer, S.; Schoels, W.; Kiehn, J. Rapid component I(Kr) of the guinea-pig cardiac delayed rectifier K(+) current is inhibited by beta(1)-adrenoreceptor activation, via cAMP/protein kinase A-dependent pathways. *Cardiovasc. Res.* **2002**, *53*, 355–362. [CrossRef] [PubMed]
14. Thomas, D.; Zhang, W.; Karle, C.A.; Kathofer, S.; Schols, W.; Kubler, W.; Kiehn, J. Deletion of protein kinase A phosphorylation sites in the HERG potassium channel inhibits activation shift by protein kinase A. *J. Biol. Chem.* **1999**, *274*, 27457–27462. [CrossRef]
15. Matsuda, H.; Cruz Jdos, S. Voltage-dependent block by internal Ca^{2+} ions of inwardly rectifying K^+ channels in guinea-pig ventricular cells. *J. Physiol.* **1993**, *470*, 295–311. [CrossRef]
16. Zaza, A.; Rocchetti, M.; Brioschi, A.; Cantadori, A.; Ferroni, A. Dynamic Ca^{2+}-induced inward rectification of K^+ current during the ventricular action potential. *Circ. Res.* **1998**, *82*, 947–956. [CrossRef]
17. Scherer, D.; Seyler, C.; Xynogalos, P.; Scholz, E.P.; Thomas, D.; Backs, J.; Andrassy, M.; Volkers, M.; Karle, C.A.; Katus, H.A.; et al. Inhibition of Cardiac Kir Current (IK1) by Protein Kinase C Critically Depends on PKCbeta and Kir2.2. *PLoS ONE* **2016**, *11*, e0156181. [CrossRef]
18. Li, J.; Marionneau, C.; Zhang, R.; Shah, V.; Hell, J.W.; Nerbonne, J.M.; Anderson, M.E. Calmodulin kinase II inhibition shortens action potential duration by upregulation of K^+ currents. *Circ. Res.* **2006**, *99*, 1092–1099. [CrossRef]
19. Wagner, S.; Hacker, E.; Grandi, E.; Weber, S.L.; Dybkova, N.; Sossalla, S.; Sowa, T.; Fabritz, L.; Kirchhof, P.; Bers, D.M.; et al. Ca/calmodulin kinase II differentially modulates potassium currents. *Circ. Arrhythm. Electrophysiol.* **2009**, *2*, 285–294. [CrossRef]
20. Nagy, N.; Acsai, K.; Kormos, A.; Sebok, Z.; Farkas, A.S.; Jost, N.; Nanasi, P.P.; Papp, J.G.; Varro, A.; Toth, A. [Ca(2+)] i-induced augmentation of the inward rectifier potassium current (IK1) in canine and human ventricular myocardium. *Pflug. Arch. Eur. J. Physiol.* **2013**, *465*, 1621–1635. [CrossRef]
21. Ni, H.; Morotti, S.; Zhang, X.; Dobrev, D.; Grandi, E. Integrative human atrial modelling unravels interactive protein kinase A and Ca^{2+}/calmodulin-dependent protein kinase II signalling as key determinants of atrial arrhythmogenesis. *Cardiovasc. Res.* **2023**, *119*, 2294–2311. [CrossRef] [PubMed]
22. Jost, N.; Acsai, K.; Horvath, B.; Banyasz, T.; Baczko, I.; Bitay, M.; Bogats, G.; Nanasi, P.P. Contribution of I Kr and I K1 to ventricular repolarization in canine and human myocytes: Is there any influence of action potential duration? *Basic Res. Cardiol.* **2009**, *104*, 33–41. [CrossRef] [PubMed]
23. Jost, N.; Virag, L.; Comtois, P.; Ordog, B.; Szuts, V.; Seprenyi, G.; Bitay, M.; Kohajda, Z.; Koncz, I.; Nagy, N.; et al. Ionic mechanisms limiting cardiac repolarization reserve in humans compared to dogs. *J. Physiol.* **2013**, *591*, 4189–4206. [CrossRef]
24. Horvath, B.; Kiss, D.; Dienes, C.; Hezso, T.; Kovacs, Z.; Szentandrassy, N.; Almassy, J.; Magyar, J.; Banyasz, T.; Nanasi, P.P. Ion current profiles in canine ventricular myocytes obtained by the "onion peeling" technique. *J. Mol. Cell. Cardiol.* **2021**, *158*, 153–162. [CrossRef]
25. Szabo, G.; Szentandrassy, N.; Biro, T.; Toth, B.I.; Czifra, G.; Magyar, J.; Banyasz, T.; Varro, A.; Kovacs, L.; Nanasi, P.P. Asymmetrical distribution of ion channels in canine and human left-ventricular wall: Epicardium versus midmyocardium. *Pflug. Arch. Eur. J. Physiol.* **2005**, *450*, 307–316. [CrossRef] [PubMed]
26. Gutierrez, D.A.; Fernandez-Tenorio, M.; Ogrodnik, J.; Niggli, E. NO-dependent CaMKII activation during beta-adrenergic stimulation of cardiac muscle. *Cardiovasc. Res.* **2013**, *100*, 392–401. [CrossRef]
27. Gomez, R.; Caballero, R.; Barana, A.; Amoros, I.; Calvo, E.; Lopez, J.A.; Klein, H.; Vaquero, M.; Osuna, L.; Atienza, F.; et al. Nitric oxide increases cardiac IK1 by nitrosylation of cysteine 76 of Kir2.1 channels. *Circ. Res.* **2009**, *105*, 383–392. [CrossRef]

28. Power, A.S.; Asamudo, E.U.; Worthington, L.P.I.; Alim, C.C.; Parackal, R.E.; Wallace, R.S.; Ebenebe, O.V.; Heller Brown, J.; Kohr, M.J.; Bers, D.M.; et al. Nitric Oxide Modulates Ca(2+) Leak and Arrhythmias via S-Nitrosylation of CaMKII. *Circ. Res.* **2023**, *133*, 1040–1055. [CrossRef]
29. Pereira, L.; Metrich, M.; Fernandez-Velasco, M.; Lucas, A.; Leroy, J.; Perrier, R.; Morel, E.; Fischmeister, R.; Richard, S.; Benitah, J.P.; et al. The cAMP binding protein Epac modulates Ca^{2+} sparks by a Ca^{2+}/calmodulin kinase signalling pathway in rat cardiac myocytes. *J. Physiol.* **2007**, *583*, 685–694. [CrossRef]
30. Oestreich, E.A.; Wang, H.; Malik, S.; Kaproth-Joslin, K.A.; Blaxall, B.C.; Kelley, G.G.; Dirksen, R.T.; Smrcka, A.V. Epac-mediated activation of phospholipase C(epsilon) plays a critical role in beta-adrenergic receptor-dependent enhancement of Ca^{2+} mobilization in cardiac myocytes. *J. Biol. Chem.* **2007**, *282*, 5488–5495. [CrossRef]
31. Oestreich, E.A.; Malik, S.; Goonasekera, S.A.; Blaxall, B.C.; Kelley, G.G.; Dirksen, R.T.; Smrcka, A.V. Epac and phospholipase Cepsilon regulate Ca^{2+} release in the heart by activation of protein kinase Cepsilon and calcium-calmodulin kinase II. *J. Biol. Chem.* **2009**, *284*, 1514–1522. [CrossRef] [PubMed]
32. Pereira, L.; Bare, D.J.; Galice, S.; Shannon, T.R.; Bers, D.M. beta-Adrenergic induced SR Ca(2+) leak is mediated by an Epac-NOS pathway. *J. Mol. Cell. Cardiol.* **2017**, *108*, 8–16. [CrossRef] [PubMed]
33. Nibley, P.C.; Shenoy, S.K. beta-adrenergic receptor signaling mediated by beta-arrestins and its potential role in heart failure. *Curr Opin Physiol* **2024**, *37*, 100723. [CrossRef] [PubMed]
34. Banyasz, T.; Horvath, B.; Virag, L.; Barandi, L.; Szentandrassy, N.; Harmati, G.; Magyar, J.; Marangoni, S.; Zaza, A.; Varro, A.; et al. Reverse rate dependency is an intrinsic property of canine cardiac preparations. *Cardiovasc. Res.* **2009**, *84*, 237–244. [CrossRef] [PubMed]
35. Hegyi, B.; Bossuyt, J.; Ginsburg, K.S.; Mendoza, L.M.; Talken, L.; Ferrier, W.T.; Pogwizd, S.M.; Izu, L.T.; Chen-Izu, Y.; Bers, D.M. Altered Repolarization Reserve in Failing Rabbit Ventricular Myocytes: Calcium and beta-Adrenergic Effects on Delayed- and Inward-Rectifier Potassium Currents. *Circ. Arrhythm. Electrophysiol.* **2018**, *11*, e005852. [CrossRef] [PubMed]
36. Hilgemann, D.W.; Ball, R. Regulation of cardiac Na+,Ca2+ exchange and KATP potassium channels by PIP2. *Science* **1996**, *273*, 956–959. [CrossRef] [PubMed]
37. Hilgemann, D.W.; Feng, S.; Nasuhoglu, C. The complex and intriguing lives of PIP2 with ion channels and transporters. *Sci. STKE* **2001**, *2001*, re19. [CrossRef] [PubMed]
38. Xu, J.X.; Si, M.; Zhang, H.R.; Chen, X.J.; Zhang, X.D.; Wang, C.; Du, X.N.; Zhang, H.L. Phosphoinositide kinases play key roles in norepinephrine- and angiotensin II-induced increase in phosphatidylinositol 4,5-bisphosphate and modulation of cardiac function. *J. Biol. Chem.* **2014**, *289*, 6941–6948. [CrossRef] [PubMed]
39. Penn, R.B.; Parent, J.L.; Pronin, A.N.; Panettieri, R.A., Jr.; Benovic, J.L. Pharmacological inhibition of protein kinases in intact cells: Antagonism of beta adrenergic receptor ligand binding by H-89 reveals limitations of usefulness. *J. Pharmacol. Exp. Ther.* **1999**, *288*, 428–437.
40. Volders, P.G.; Stengl, M.; van Opstal, J.M.; Gerlach, U.; Spatjens, R.L.; Beekman, J.D.; Sipido, K.R.; Vos, M.A. Probing the contribution of IKs to canine ventricular repolarization: Key role for beta-adrenergic receptor stimulation. *Circulation* **2003**, *107*, 2753–2760. [CrossRef]
41. Stengl, M.; Volders, P.G.; Thomsen, M.B.; Spatjens, R.L.; Sipido, K.R.; Vos, M.A. Accumulation of slowly activating delayed rectifier potassium current (IKs) in canine ventricular myocytes. *J. Physiol.* **2003**, *551*, 777–786. [CrossRef] [PubMed]
42. Horvath, B.; Vaczi, K.; Hegyi, B.; Gonczi, M.; Dienes, B.; Kistamas, K.; Banyasz, T.; Magyar, J.; Baczko, I.; Varro, A.; et al. Sarcolemmal Ca(2+)-entry through L-type Ca(2+) channels controls the profile of Ca(2+)-activated Cl(-) current in canine ventricular myocytes. *J. Mol. Cell. Cardiol.* **2016**, *97*, 125–139. [CrossRef] [PubMed]
43. Horvath, B.; Hezso, T.; Szentandrassy, N.; Kistamas, K.; Arpadffy-Lovas, T.; Varga, R.; Gazdag, P.; Veress, R.; Dienes, C.; Baranyai, D.; et al. Late sodium current in human, canine and guinea pig ventricular myocardium. *J. Mol. Cell. Cardiol.* **2020**, *139*, 14–23. [CrossRef] [PubMed]
44. Banyasz, T.; Magyar, J.; Szentandrassy, N.; Horvath, B.; Birinyi, P.; Szentmiklosi, J.; Nanasi, P.P. Action potential clamp fingerprints of K^+ currents in canine cardiomyocytes: Their role in ventricular repolarization. *Acta Physiol.* **2007**, *190*, 189–198. [CrossRef] [PubMed]
45. Bányász, T.; Fülöp, L.; Magyar, J.; Szentandrássy, N.; Varró, A.; Nánási, P.P. Endocardial versus epicardial differences in L-type calcium current in canine ventricular myocytes studied by action potential voltage clamp. *Cardiovasc. Res.* **2003**, *58*, 66–75. [CrossRef]
46. Hegyi, B.; Chen-Izu, Y.; Jian, Z.; Shimkunas, R.; Izu, L.T.; Banyasz, T. KN-93 inhibits IKr in mammalian cardiomyocytes. *J. Mol. Cell. Cardiol.* **2015**, *89*, 173–176. [CrossRef]

Disclaimer/Publisher's Note: The statements, opinions and data contained in all publications are solely those of the individual author(s) and contributor(s) and not of MDPI and/or the editor(s). MDPI and/or the editor(s) disclaim responsibility for any injury to people or property resulting from any ideas, methods, instructions or products referred to in the content.